DESY–00–017

February 2000

The Q^2 Dependence of Dijet Cross Sections in γp Interactions at HERA

ZEUS Collaboration

Abstract

The dependence of the photon structure on the photon virtuality, Q^2, is studied by measuring the reaction $e^+p \to e^+ +$ jet+ jet+ X at photon-proton centre-of-mass energies $134 < W < 223$ GeV. Events have been selected in the Q^2 ranges ≈ 0 GeV^2, 0.1-0.55 GeV^2, and 1.5-4.5 GeV^2, having two jets with transverse energy $E_T^{jet} > 5.5$ GeV in the final state. The dijet cross section has been measured as a function of the fractional momentum of the photon participating in the hard process, $x_\gamma^{\rm OBS}$. The ratio of the dijet cross section with $x_\gamma^{\rm OBS} < 0.75$ to that with $x_\gamma^{\rm OBS} > 0.75$ decreases as Q^2 increases. The data are compared with the predictions of NLO pQCD and leading-order Monte Carlo programs using various parton distribution functions of the photon. The measurements can be interpreted in terms of a resolved photon component that falls with Q^2 but remains present at values of Q^2 up to 4.5 GeV^2. However, none of the models considered gives a good description of the data.

The ZEUS Collaboration

J. Breitweg, S. Chekanov, M. Derrick, D. Krakauer, S. Magill, B. Musgrave, A. Pellegrino, J. Repond, R. Stanek, R. Yoshida
Argonne National Laboratory, Argonne, IL, USA [p]

M.C.K. Mattingly
Andrews University, Berrien Springs, MI, USA

G. Abbiendi, F. Anselmo, P. Antonioli, G. Bari, M. Basile, L. Bellagamba, D. Boscherini[1], A. Bruni, G. Bruni, G. Cara Romeo, G. Castellini[2], L. Cifarelli[3], F. Cindolo, A. Contin, N. Coppola, M. Corradi, S. De Pasquale, P. Giusti, G. Iacobucci, G. Laurenti, G. Levi, A. Margotti, T. Massam, R. Nania, F. Palmonari, A. Pesci, A. Polini, G. Sartorelli, Y. Zamora Garcia[4], A. Zichichi
University and INFN Bologna, Bologna, Italy [f]

C. Amelung, A. Bornheim, I. Brock, K. Coböken, J. Crittenden, R. Deffner, H. Hartmann, K. Heinloth, E. Hilger, P. Irrgang, H.-P. Jakob, A. Kappes, U.F. Katz, R. Kerger, E. Paul, H. Schnurbusch,
A. Stifutkin, J. Tandler, K.Ch. Voss, A. Weber, H. Wieber
Physikalisches Institut der Universität Bonn, Bonn, Germany [c]

D.S. Bailey, O. Barret, N.H. Brook[5], B. Foster[6], G.P. Heath, H.F. Heath, J.D. McFall, D. Piccioni, E. Rodrigues, J. Scott, R.J. Tapper
H.H. Wills Physics Laboratory, University of Bristol, Bristol, U.K. [o]

M. Capua, A. Mastroberardino, M. Schioppa, G. Susinno
Calabria University, Physics Dept.and INFN, Cosenza, Italy [f]

H.Y. Jeoung, J.Y. Kim, J.H. Lee, I.T. Lim, K.J. Ma, M.Y. Pac[7]
Chonnam National University, Kwangju, Korea [h]

A. Caldwell, W. Liu, X. Liu, B. Mellado, S. Paganis, R. Sacchi, S. Sampson, F. Sciulli
Columbia University, Nevis Labs., Irvington on Hudson, N.Y., USA [q]

J. Chwastowski, A. Eskreys, J. Figiel, K. Klimek, K. Olkiewicz, K. Piotrzkowski[8], M.B. Przybycień, P. Stopa, L. Zawiejski
Inst. of Nuclear Physics, Cracow, Poland [j]

L. Adamczyk, B. Bednarek, K. Jeleń, D. Kisielewska, A.M. Kowal, T. Kowalski, M. Przybycień,
E. Rulikowska-Zarębska, L. Suszycki, D. Szuba
Faculty of Physics and Nuclear Techniques, Academy of Mining and Metallurgy, Cracow, Poland [j]

A. Kotański
Jagellonian Univ., Dept. of Physics, Cracow, Poland [k]

L.A.T. Bauerdick, U. Behrens, J.K. Bienlein, C. Burgard[9], K. Desler, G. Drews, A. Fox-Murphy, U. Fricke, F. Goebel, P. Göttlicher, R. Graciani, T. Haas, W. Hain, G.F. Hartner, D. Hasell[10], K. Hebbel, K.F. Johnson[11], M. Kasemann[12], W. Koch, U. Kötz, H. Kowalski, L. Lindemann[13], B. Löhr, M. Martínez, M. Milite, T. Monteiro[8], M. Moritz, D. Notz, F. Pelucchi, M.C. Petrucci, M. Rohde, P.R.B. Saull, A.A. Savin, U. Schneekloth, F. Selonke, M. Sievers, S. Stonjek, E. Tassi, G. Wolf, U. Wollmer, C. Youngman, W. Zeuner
Deutsches Elektronen-Synchrotron DESY, Hamburg, Germany

C. Coldewey, H.J. Grabosch, A. Lopez-Duran Viani, A. Meyer, S. Schlenstedt, P.B. Straub
DESY Zeuthen, Zeuthen, Germany

G. Barbagli, E. Gallo, P. Pelfer
University and INFN, Florence, Italy [f]

G. Maccarrone, L. Votano
INFN, Laboratori Nazionali di Frascati, Frascati, Italy [f]

A. Bamberger, A. Benen, S. Eisenhardt[14], P. Markun, H. Raach, S. Wölfle
Fakultät für Physik der Universität Freiburg i.Br., Freiburg i.Br., Germany [c]

P.J. Bussey, A.T. Doyle, S.W. Lee, N. Macdonald, G.J. McCance, D.H. Saxon, L.E. Sinclair, I.O. Skillicorn, R. Waugh
Dept. of Physics and Astronomy, University of Glasgow, Glasgow, U.K. [o]

I. Bohnet, N. Gendner, U. Holm, A. Meyer-Larsen, H. Salehi, K. Wick
Hamburg University, I. Institute of Exp. Physics, Hamburg, Germany [c]

D. Dannheim, A. Garfagnini, I. Gialas[15], L.K. Gladilin[16], D. Kçira[17], R. Klanner, E. Lohrmann, G. Poelz, F. Zetsche
Hamburg University, II. Institute of Exp. Physics, Hamburg, Germany [c]

R. Goncalo, K.R. Long, D.B. Miller, A.D. Tapper, R. Walker
Imperial College London, High Energy Nuclear Physics Group, London, U.K. [o]

U. Mallik
University of Iowa, Physics and Astronomy Dept., Iowa City, USA [p]

P. Cloth, D. Filges
Forschungszentrum Jülich, Institut für Kernphysik, Jülich, Germany

T. Ishii, M. Kuze, K. Nagano, K. Tokushuku[18], S. Yamada, Y. Yamazaki
Institute of Particle and Nuclear Studies, KEK, Tsukuba, Japan [g]

S.H. Ahn, S.H. An, S.J. Hong, S.B. Lee, S.W. Nam[19], S.K. Park
Korea University, Seoul, Korea [h]

H. Lim, I.H. Park, D. Son
Kyungpook National University, Taegu, Korea [h]

F. Barreiro, G. García, C. Glasman[20], O. Gonzalez, L. Labarga, J. del Peso, I. Redondo[21], J. Terrón
Univer. Autónoma Madrid, Depto de Física Teórica, Madrid, Spain [n]

M. Barbi, F. Corriveau, D.S. Hanna, A. Ochs, S. Padhi, M. Riveline, D.G. Stairs, M. Wing
McGill University, Dept. of Physics, Montréal, Québec, Canada [a], [b]

T. Tsurugai
Meiji Gakuin University, Faculty of General Education, Yokohama, Japan

V. Bashkirov[22], B.A. Dolgoshein
Moscow Engineering Physics Institute, Moscow, Russia [l]

R.K. Dementiev, P.F. Ermolov, Yu.A. Golubkov, I.I. Katkov, L.A. Khein, N.A. Korotkova, I.A. Korzhavina, V.A. Kuzmin, O.Yu. Lukina, A.S. Proskuryakov, L.M. Shcheglova, A.N. Solomin,
N.N. Vlasov, S.A. Zotkin
Moscow State University, Institute of Nuclear Physics, Moscow, Russia [m]

C. Bokel, M. Botje, N. Brümmer, J. Engelen, S. Grijpink, E. Koffeman, P. Kooijman, S. Schagen, A. van Sighem, H. Tiecke, N. Tuning, J.J. Velthuis, J. Vossebeld, L. Wiggers, E. de Wolf
NIKHEF and University of Amsterdam, Amsterdam, Netherlands [i]

B. Bylsma, L.S. Durkin, J. Gilmore, C.M. Ginsburg, C.L. Kim, T.Y. Ling, P. Nylander[23]
Ohio State University, Physics Department, Columbus, Ohio, USA [p]

S. Boogert, A.M. Cooper-Sarkar, R.C.E. Devenish, J. Große-Knetter[24], T. Matsushita, O. Ruske,
M.R. Sutton, R. Walczak
Department of Physics, University of Oxford, Oxford U.K. [o]

A. Bertolin, R. Brugnera, R. Carlin, F. Dal Corso, U. Dosselli, S. Dusini, S. Limentani, M. Morandin, M. Posocco, L. Stanco, R. Stroili, C. Voci
Dipartimento di Fisica dell' Università and INFN, Padova, Italy [f]

L. Iannotti[25], B.Y. Oh, J.R. Okrasiński, W.S. Toothacker, J.J. Whitmore
Pennsylvania State University, Dept. of Physics, University Park, PA, USA [q]

Y. Iga
Polytechnic University, Sagamihara, Japan [g]

G. D'Agostini, G. Marini, A. Nigro
Dipartimento di Fisica, Univ. 'La Sapienza' and INFN, Rome, Italy [f]

C. Cormack, J.C. Hart, N.A. McCubbin, T.P. Shah
Rutherford Appleton Laboratory, Chilton, Didcot, Oxon, U.K. [o]

D. Epperson, C. Heusch, H.F.-W. Sadrozinski, A. Seiden, R. Wichmann, D.C. Williams
University of California, Santa Cruz, CA, USA [p]

N. Pavel
Fachbereich Physik der Universität-Gesamthochschule Siegen, Germany [c]

H. Abramowicz[26], S. Dagan[27], S. Kananov[27], A. Kreisel, A. Levy[27]
Raymond and Beverly Sackler Faculty of Exact Sciences, School of Physics, Tel-Aviv University,
Tel-Aviv, Israel [e]

T. Abe, T. Fusayasu, K. Umemori, T. Yamashita
Department of Physics, University of Tokyo, Tokyo, Japan [g]

R. Hamatsu, T. Hirose, M. Inuzuka, S. Kitamura[28], T. Nishimura
Tokyo Metropolitan University, Dept. of Physics, Tokyo, Japan [g]

M. Arneodo[29], N. Cartiglia, R. Cirio, M. Costa, M.I. Ferrero, S. Maselli, V. Monaco, C. Peroni, M. Ruspa, A. Solano, A. Staiano
Università di Torino, Dipartimento di Fisica Sperimentale and INFN, Torino, Italy [f]

M. Dardo
II Faculty of Sciences, Torino University and INFN - Alessandria, Italy [f]

D.C. Bailey, C.-P. Fagerstroem, R. Galea, T. Koop, G.M. Levman, J.F. Martin, R.S. Orr, S. Polenz, A. Sabetfakhri, D. Simmons
University of Toronto, Dept. of Physics, Toronto, Ont., Canada [a]

J.M. Butterworth, C.D. Catterall, M.E. Hayes, E.A. Heaphy, T.W. Jones, J.B. Lane, B.J. West
University College London, Physics and Astronomy Dept., London, U.K. [o]

J. Ciborowski, R. Ciesielski, G. Grzelak, R.J. Nowak, J.M. Pawlak, R. Pawlak, B. Smalska, T. Tymieniecka, A.K. Wróblewski, J.A. Zakrzewski, A.F. Żarnecki
Warsaw University, Institute of Experimental Physics, Warsaw, Poland [j]

M. Adamus, T. Gadaj
Institute for Nuclear Studies, Warsaw, Poland [j]

O. Deppe, Y. Eisenberg[27], D. Hochman, U. Karshon[27]
Weizmann Institute, Department of Particle Physics, Rehovot, Israel [d]

W.F. Badgett, D. Chapin, R. Cross, C. Foudas, S. Mattingly, D.D. Reeder, W.H. Smith, A. Vaiciulis[30], T. Wildschek, M. Wodarczyk
University of Wisconsin, Dept. of Physics, Madison, WI, USA [p]

A. Deshpande, S. Dhawan, V.W. Hughes
Yale University, Department of Physics, New Haven, CT, USA [p]

S. Bhadra, J.E. Cole, W.R. Frisken, R. Hall-Wilton, M. Khakzad, S. Menary, W.B. Schmidke
York University, Dept. of Physics, Toronto, Ont., Canada [a]

[1] now visiting scientist at DESY
[2] also at IROE Florence, Italy
[3] now at Univ. of Salerno and INFN Napoli, Italy
[4] supported by Worldlab, Lausanne, Switzerland
[5] PPARC Advanced fellow
[6] also at University of Hamburg, Alexander von Humboldt Research Award
[7] now at Dongshin University, Naju, Korea
[8] now at CERN
[9] now at Barclays Capital PLC, London
[10] now at Massachusetts Institute of Technology, Cambridge, MA, USA
[11] visitor from Florida State University
[12] now at Fermilab, Batavia, IL, USA
[13] now at SAP A.G., Walldorf, Germany
[14] now at University of Edinburgh, Edinburgh, U.K.
[15] visitor of Univ. of Crete, Greece, partially supported by DAAD, Bonn - Kz. A/98/16764
[16] on leave from MSU, supported by the GIF, contract I-0444-176.07/95
[17] supported by DAAD, Bonn - Kz. A/98/12712
[18] also at University of Tokyo
[19] now at Wayne State University, Detroit
[20] supported by an EC fellowship number ERBFMBICT 972523
[21] supported by the Comunidad Autonoma de Madrid
[22] now at Loma Linda University, Loma Linda, CA, USA
[23] now at Hi Techniques, Inc., Madison, WI, USA
[24] supported by the Feodor Lynen Program of the Alexander von Humboldt foundation
[25] partly supported by Tel Aviv University
[26] an Alexander von Humboldt Fellow at University of Hamburg
[27] supported by a MINERVA Fellowship
[28] present address: Tokyo Metropolitan University of Health Sciences, Tokyo 116-8551, Japan
[29] now also at Università del Piemonte Orientale, I-28100 Novara, Italy
[30] now at University of Rochester, Rochester, NY, USA

[a] supported by the Natural Sciences and Engineering Research Council of Canada (NSERC)
[b] supported by the FCAR of Québec, Canada
[c] supported by the German Federal Ministry for Education and Science, Research and Technology (BMBF), under contract numbers 057BN19P, 057FR19P, 057HH19P, 057HH29P, 057SI75I
[d] supported by the MINERVA Gesellschaft für Forschung GmbH, the German Israeli Foundation, and by the Israel Ministry of Science
[e] supported by the German-Israeli Foundation, the Israel Science Foundation, the U.S.-Israel Binational Science Foundation, and by the Israel Ministry of Science
[f] supported by the Italian National Institute for Nuclear Physics (INFN)
[g] supported by the Japanese Ministry of Education, Science and Culture (the Monbusho) and its grants for Scientific Research
[h] supported by the Korean Ministry of Education and Korea Science and Engineering Foundation
[i] supported by the Netherlands Foundation for Research on Matter (FOM)
[j] supported by the Polish State Committee for Scientific Research, grant No. 112/E-356/SPUB/DESY/P03/DZ 3/99, 620/E-77/SPUB/DESY/P-03/ DZ 1/99, 2P03B03216, 2P03B04616, 2P03B03517, and by the German Federal Ministry of Education and Science, Research and Technology (BMBF)
[k] supported by the Polish State Committee for Scientific Research (grant No. 2P03B08614 and 2P03B06116)
[l] partially supported by the German Federal Ministry for Education and Science, Research and Technology (BMBF)
[m] supported by the Fund for Fundamental Research of Russian Ministry for Science and Education and by the German Federal Ministry for Education and Science, Research and Technology (BMBF)
[n] supported by the Spanish Ministry of Education and Science through funds provided by CICYT
[o] supported by the Particle Physics and Astronomy Research Council
[p] supported by the US Department of Energy
[q] supported by the US National Science Foundation

1 Introduction

The photon at high virtuality, Q^2, is commonly considered to be a point-like probe of the structure of a particular hadronic target [1]. However, the real photon ($Q^2 \approx 0$ GeV^2) has itself a partonic structure, which has been studied in two-photon reactions from e^+e^- scattering [2], and in jet production at HERA [3, 4]. In this paper, the transition between the real photon and the virtual photon is investigated for $0 \leq Q^2 \leq 4.5$ GeV^2 using dijet events in ep scattering at HERA.

The photon, in general, may have both a partonic structure and a point-like coupling to charged quarks and leptons. As a result, two types of process can contribute to jet production in γp interactions in leading order (LO) perturbative QCD (pQCD): the direct process, in which the photon couples directly to quarks at high transverse momenta, one of which scatters from a parton in the proton, and the resolved process, where a parton from the photon scatters from a parton in the proton. Conventionally, two types of resolved photon process are defined. In the first, the photon acts via an intermediate meson-like hadronic state whose description is essentially non-perturbative, so that a phenomenological parton density function must be introduced. In the second, the photon interacts initially by splitting into a $q\bar{q}$ pair at moderate transverse energy, a point-like perturbative process which is termed 'anomalous' and can in principle, for $Q^2 > 0$ GeV^2, be summed to all orders. The boundary between the two types of resolved process is factorisation-scale dependent.

At a given photon virtuality, Q^2, and hard QCD scale, μ^2, both types of resolved process can in principle occur. It is usually accepted that, at low Q^2, the hadronic type is important, while at higher Q^2, resolved processes are dominated by the anomalous type. The general expectation is that the contribution to the dijet cross section from both types of resolved photon processes should decrease relative to the contribution from direct photon processes as the virtuality of the photon increases towards μ^2, *i.e.* the partonic content of the photon becomes suppressed [5, 6, 7, 8]. The first measurements came from the PLUTO collaboration [9]. The H1 collaboration has also studied the transition between photoproduction and deep inelastic scattering by measuring, in the $\gamma^* p$ CM frame, inclusive jet cross sections for real and virtual photons [10] and dijet cross sections [11] for $Q^2 > 1.6$ GeV^2.

The resolved and direct components can be separated on the basis of the variable $x_\gamma^{\rm OBS}$, which is the fractional momentum of the photon partaking in the production of the dijet system. This variable is defined as:

$$x_\gamma^{\rm OBS} = \frac{\sum_{jets} E_T^{jet} e^{-\eta^{jet}}}{2yE_e}$$

where E_T^{jet} and η^{jet} are the transverse energy and pseudorapidity of the jet defined in the laboratory frame[1]. The variable y is defined as $y = 1 - \frac{E_e'}{2E_e}(1 - \cos\theta_e')$, where E_e is

[1]The ZEUS right-handed coordinate system is defined with the origin at the nominal interaction point by the Z axis pointing in the proton beam direction and the X axis pointing horizontally towards the centre of HERA.

the positron beam energy and $E_e^{'}$, $\theta_e^{'}$ are the energy and polar angle, respectively, of the scattered positron. Since $x_\gamma^{\rm OBS}$ is well defined at all orders in pQCD, measurements based on it can be compared with theoretical predictions at any given order.

At $x_\gamma^{\rm OBS} > 0.75$, the direct component dominates, while the $x_\gamma^{\rm OBS} < 0.75$ region is sensitive mainly to the resolved component. However, events with low values of $x_\gamma^{\rm OBS}$ can also be produced when initial- and final-state parton showers give rise to hadronic activity outside the dijet system.

Experimental $x_\gamma^{\rm OBS}$ distributions obtained from 1995 ZEUS data are presented in this paper. The ratio of the measured cross sections for $x_\gamma^{\rm OBS} < 0.75$ and > 0.75 is then given as a function of $\rm Q^2$. The values of the ratio are compared with theoretical calculations at both LO and next-to-leading-order (NLO) pQCD computed using the JetViP program [12].

2 Experimental Setup and Data Selection

During 1995, HERA operated with protons of energy $E_p = 820$ GeV and positrons of energy $E_e = 27.5$ GeV. The ZEUS detector is described in detail elsewhere [13, 14]. The main components used in the present analysis are the uranium-scintillator sampling calorimeter (CAL) [15], the beam pipe calorimeter (BPC) [16], and the central tracking chamber [17] positioned in a 1.43 T solenoidal magnetic field. The CAL energy resolution for positrons, under test beam conditions, was measured to be $0.18/\sqrt{E_e^{'}(\rm GeV)}$. The point of impact of the positron in CAL was measured with a resolution of 3 mm, resulting in a $\rm Q^2$ resolution of 8%. The systematic uncertainty on the absolute value of $E_e^{'}$ is 2%. The BPC was installed 294 cm from the interaction point in the positron direction in order to tag scattered positrons at small angles (15-34 mrad). It measured both the energy, $E_e^{'}$, of the scattered positron and the position of its impact point. The energy resolution of the BPC is $0.17/\sqrt{E_e^{'}(\rm GeV)}$ and the position resolution is 0.5 mm, resulting in a $\rm Q^2$ resolution of 6%. The systematic uncertainty on the absolute value of $E_e^{'}$ is 0.5%.

The events were selected online via a three-level trigger system [14, 18, 19] using the same selection algorithms as in a previous dijet publication [4], except that in the third-level trigger (TLT) the events were required to have at least two jets with $E_T^{TLT} > 4.0$ GeV and $\eta^{TLT} < 2.5$. The sample was separated offline into subsamples corresponding to three different $\rm Q^2$ ranges:

- Events with quasi-real photons ($\rm Q^2 \approx 0$ GeV^2, named PHP in the following) were selected by requiring that no identified positron was found in the CAL with energy $E_e^{'} > 5$ GeV [20] and $y < 0.7$. The resulting sample had $\rm Q^2 < 1.0$ GeV^2 with an estimated median of 10^{-3} GeV^2;
- Events at intermediate $\rm Q^2$ (IQS) were selected by requiring that the scattered positron was measured by the BPC. In this data set, the BPC tagged events with photon virtualities in the range $0.1 < \rm Q^2 < 0.55$ GeV^2. For this sample the energy of the scattered positron was required to be $E_e^{'} > 12.5$ GeV;

- Deep inelastic scattering (DIS) events at low Q^2 (LDIS) were selected by requiring that the outgoing positron was measured in the CAL. The energy of the scattered positron was required to satisfy $E_e^{'} > 11.0$ GeV [20] and the Q^2 range was restricted to $1.5 < Q^2 < 4.5$ GeV^2.

For all three samples, additional cuts of $0.15 < y_{JB} < 0.45$ were applied, where y_{JB} is an estimator[2] of y [21]. Due to the energy lost in the inactive material in front of the CAL and to particles lost in the rear beampipe, y_{JB} systematically underestimates the true y by approximately 20%, an effect which is adequately reproduced in the Monte Carlo simulation of the detector. The combination of y_{JB} and $E_e^{'}$ cuts ensured that all three samples corresponded to the same true y range ($0.2 < y < 0.55$).

The longitudinally invariant k_T algorithm [22], in the mode described in a previous publication [4], was then applied to the CAL cells to search for events with two jets in the final state. In the LDIS sample, the cells associated with the positron were excluded from the jet search. The two jets with the highest transverse energy were required to have pseudorapidity between $-1.125 < \eta^{jet} < 2.2$ and transverse energy $E_T^{jet} > 5.5$ GeV.

After all cuts, the jet search resulted in a sample of 58224 dijet events for the PHP sample, 353 dijet events for the IQS sample and 1172 dijet events for the LDIS sample. Approximately 10% of the events in each of the three samples had three or more jets. The PHP, IQS and LDIS samples correspond to integrated luminosities of 3.1, 3.3 and 4.9 pb^{-1}, respectively.

3 Data Corrections and Systematics

The data were corrected for acceptance, smearing and kinematic cuts using the HERWIG 5.9 [23] Monte Carlo (MC) model. Leading-order resolved (LO-RES) and direct (LO-DIR) processes were generated separately. Resolved photon events were generated not only in the PHP, but also in the IQS and LDIS regimes. The minimum transverse momentum of the partonic hard scatter ($\hat{p}_T^{\min}$) was set to 2.5 GeV. The GRV LO [24] and the MRSA [25] sets were used for the photon and proton parton distribution functions (PDF), respectively. To simulate possible interactions between the proton and photon remnants ('underlying event'), the option of multiparton interactions (MI) [26, 27] was included for the PHP sample. It has been shown that the simulation of the underlying event with MI improves the description of the energy flow around the jet axis for jet production from quasi-real photon-proton interactions [4].

The Monte Carlo events were processed through the full ZEUS detector simulation using the same cuts as applied to the data. The normalisations of the LO-RES and LO-DIR processes were extracted from the data using a two-parameter fit to the uncorrected $x_\gamma^{\rm OBS}$ distributions. This procedure was applied separately for each Q^2 range.

[2] $y_{JB} = \sum_i (E_i - E_{Zi})/2E_e$, where $E_{Zi} = E_i \cos\theta_i$ and E_i is the energy deposited in the CAL cell i which has a polar angle θ_i with respect to the measured Z-vertex of the event. The sum runs over all CAL cells excluding those associated with a detected scattered positron.

Figure 1 shows uncorrected distributions of $x_\gamma^{\rm OBS}$ for PHP, IQS, and LDIS dijet events compared with the HERWIG simulation. Events both at high $x_\gamma^{\rm OBS}$, associated mainly with direct photon processes, and at low $x_\gamma^{\rm OBS}$, associated mainly with the resolved photon processes, are present in all Q^2 ranges.

In the low $x_\gamma^{\rm OBS}$ region, the PHP data disagree with the simulation. Disagreement is also observed in the η^{jet}, y_{JB}, and E_T^{jet} distributions (not shown) and can be attributed to the presence of underlying event effects or uncertainty in the PDFs of the photon. The underlying event effects are most evident at low $x_\gamma^{\rm OBS}$ and low E_T^{jet}. For the combination of $\hat{p}_T^{\rm min}$ and photon PDF used here, the simulation of multiparton interactions does not reproduce the shape of the data in the low $x_\gamma^{\rm OBS}$ region [4]. To take account of this disagreement in the correction of the data for migrations and acceptance, the Monte Carlo events have been reweighted as a function of $x_\gamma^{\rm OBS}$ at the hadron level so that the distribution agrees with the data. The result of the reweighting is shown in Fig. 1 (a). After the reweighting, the MC predictions for the η^{jet}, y_{JB}, and E_T^{jet} distributions also agree well with the data (not shown).

The dijet differential cross sections, $d\sigma/dx_\gamma^{\rm OBS}$, corrected to the hadron level, have been measured using the k_T jet algorithm, in the three Q^2 regions with $0.2 < y < 0.55$. The measurements have been made for two sets of jet transverse energy and pseudorapidity cuts:

1. Low E_T^{jet}: $E_T^{jet} > 5.5$ GeV, $-1.125 < \eta^{jet} < 2.2$ for both jets;
2. High E_T^{jet}: $E_T^{jet_1} > 7.5$ GeV, $E_T^{jet_2} > 6.5$ GeV, $-1.125 < \eta^{jet} < 1.875$.

The data with the low set of E_T^{jet} cuts are sensitive to the resolved photon component, but also to the effects of the underlying event. The data with the high E_T^{jet} cuts are not significantly influenced by the underlying event effects; this was established by means of a comparison (not shown) of the data with HERWIG without MI. The high E_T^{jet} cuts were chosen to be asymmetrical to facilitate a comparison with the NLO pQCD calculation.

The cross sections at hadron level were obtained by applying a bin-by-bin correction to the measured dijet distributions binned in four $x_\gamma^{\rm OBS}$ bins (0.0625-0.25, 0.25-0.50, 0.50-0.75, 0.75-1.00) and four Q^2 bins (0.-1.0, 0.1-0.55, 1.5-3.0, 3.0-4.5 GeV^2). The correction factors take into account the efficiency of the trigger, the selection criteria and the purity and efficiency of the jet reconstruction. The efficiency and purity are determined as a function of $x_\gamma^{\rm OBS}$ and Q^2 from the MC simulation [28]. In the PHP region, the correction factors lie between 1.25-1.43 and the purities between 0.50-0.64. In the IQS region, the correction factors are dominated by the BPC geometric acceptance and lie between 17.6-23.0 and the purities between 0.40-0.70. For the LDIS region the correction factors lie between 3.1-3.8, and the purities between 0.45 and 0.80.

A detailed study of the systematic uncertainties of the measurements has been performed [29, 30]. The uncertainties have been separated into those that are uncorrelated and therefore were added in quadrature to the statistical error and those that are correlated and presented separately. The uncorrelated systematic uncertainties originate from the residual uncertainties in the event simulation. The uncertainty associated with the E_T^{jet}

cut is the dominant uncorrelated uncertainty for the PHP and IQS samples. When this cut is varied by the E_T^{jet} resolution of 14%, a systematic uncertainty between -9% and $+12\%$ results, except for $x_\gamma^{\rm OBS} < 0.25$ in the IQS region where the uncertainty ranges between -28% and $+10\%$. In the LDIS region, the dominant systematic uncertainty comes from the uncertainty in $x_\gamma^{\rm OBS}$ (the $x_\gamma^{\rm OBS}$ resolution is 0.05) and results in a systematic error between -2% and $+6\%$, except for $x_\gamma^{\rm OBS} < 0.25$ where the systematic uncertainty ranges between -25% and $+36\%$.

Two sources of correlated systematic uncertainties have been studied, one originating from the uncertainty of the CAL energy scale and the other from the use of different models for the description of the jet fragmentation process in the MC. The absolute energy scale of the jets in simulated events has been varied by $\pm 5\%$ [31]. The effect of this variation on the dijet cross sections is $\approx \pm 20\%$. The uncertainty associated with the jet fragmentation was studied by correcting the data to the hadron level using PYTHIA [32] and comparing to the results obtained using HERWIG. The effect was estimated to be on average $\sim 20\%$. In addition, there is an overall normalisation uncertainty of 1.5% from the luminosity determination, which is not included.

4 Results and Discussion

The $x_\gamma^{\rm OBS}$ distributions shown in Fig. 1, in all three $\rm Q^2$ ranges, cannot be described by HERWIG without including a significant LO resolved photon component, which is dominant for $x_\gamma^{\rm OBS} < 0.75$. Hence the dijet cross sections in this region are sensitive to the photon structure.

The measured dijet cross sections for the low and the high E_T^{jet} cuts described in Section 3 are shown in Figs. 2 and 3, respectively. The shapes of the dijet cross sections change markedly with increasing $\rm Q^2$, the cross section in the low-$x_\gamma^{\rm OBS}$ region decreasing faster than the cross section in the high-$x_\gamma^{\rm OBS}$ region. This effect is more pronounced for the low E_T^{jet} cuts.

The dijet cross sections are compared to the predictions of the HERWIG MC at hadron level using different photon PDFs. Those of GRV LO [24] and WHIT2 [33] are valid for real photons only, have differing gluon distributions and have no suppression of the resolved photon component as $\rm Q^2$ increases. In the SaS 1D [5] model the resolved photon consists of two separate contributions, the non-perturbative hadronic 'Vector Meson Dominance' component and the anomalous pQCD component, each with different $\rm Q^2$ dependence. Specifically, the 'Vector Meson Dominance' component of the resolved photon is predicted to decrease approximately as $(m_\rho^2/(m_\rho^2 + \rm Q^2))^2$. The pQCD component is predicted to decrease more slowly as $\sim \log(\mu^2/\rm Q^2)$, where μ^2 is the hard QCD scale of the process which, for jet production, is usually taken to be proportional to $\left(E_T^{jet}\right)^2$. The measured cross sections for the LDIS region are also compared to the LEPTO [34] Monte Carlo prediction, which does not include a resolved photon component and uses a parton-shower model to account for higher-order pQCD effects. The general framework is similar to the LO-DIR HERWIG and PYTHIA simulations. In this picture, the dijet cross section at low $x_\gamma^{\rm OBS}$ arises purely from parton-shower contributions to the LO-DIR

process. The HERWIG and LEPTO predictions agree in the highest $x_\gamma^{\rm OBS}$ bin, where the direct component dominates. In order to compare the shape of the measured cross sections with that of the MC predictions, the latter have been normalized to the data cross sections for $x_\gamma^{\rm OBS} > 0.75$.

The low E_T^{jet} cross sections are compared to the HERWIG predictions in Fig. 2. The SaS 1D prediction without MI agrees qualitatively with the data in the LDIS range; however a disagreement is observed at low $x_\gamma^{\rm OBS}$ in the IQS and PHP ranges, which becomes more striking as Q^2 decreases. The GRV prediction without MI and the WHIT2 prediction both without and with MI using $\hat{p}_T^{\rm min} = 2.0$ GeV are compared to the data in the PHP region, where the discrepancy with SaS 1D is greatest. The effect of MI is found to be very sensitive to the $\hat{p}_T^{\rm min}$ value and to the choice of PDF [27, 35]. The model using WHIT2 with MI gives reasonable agreement with the data. The shape of the low E_T^{jet}-cut cross sections, shown in Fig. 2 (a), cannot be described by the models that do not include MI. The discrepancy seen for the PHP data using SaS 1D without MI is not present in the LDIS region. This is as expected, in the framework of the MI model, if the resolved component decreases with Q^2. The LEPTO predictions underestimate the dijet cross sections at low $x_\gamma^{\rm OBS}$ in the LDIS region, indicating that the parton-shower contributions alone cannot describe the dijet data in this region.

The high-E_T^{jet} data are shown in Fig. 3. The predictions of HERWIG without multi-parton interactions using the SaS 1D photon PDF describe the shape of the measured cross section well in the LDIS region but tend to underestimate the PHP and IQS data at low $x_\gamma^{\rm OBS}$. The measurements are also compared to HERWIG using GRV without MI. This model is in good agreement with the data in the PHP and IQS regions but fails to describe the data in the LDIS region, as expected since the GRV set describing the real photon structure is used. As seen in Fig. 3 (c), LEPTO again underestimates the dijet cross sections at low $x_\gamma^{\rm OBS}$.

The cross-section ratio $\sigma(x_\gamma^{\rm OBS} < 0.75)/\sigma(x_\gamma^{\rm OBS} > 0.75)$ as a function of Q^2 for both sets of E_T^{jet} cuts is shown in Fig. 4. The dominant systematic uncertainties of these measurements (7-16%) are due to the E_T^{jet} and $x_\gamma^{\rm OBS}$ cuts, except for the LDIS samples where the cut on the impact point of the scattered positron results in an additional systematic uncertainty of about 10%. For the IQS measurements, the latter systematic uncertainty falls to 5%. When the data are corrected using PYTHIA, the measured ratios are systematically lower for all Q^2 points. This systematic error is therefore not included with the previous ones, but it is shown separately. For the PHP data, there is an additional error of 5% due to uncertainties in the Monte Carlo normalisation factors for the LO-DIR and LO-RES used in the fit (not shown).

The cross-section ratio falls steeply as a function of Q^2. This can be interpreted as the suppression of the resolved photon component as the photon virtuality increases. The decrease is more pronounced for the measurements using the low set of E_T^{jet} cuts, which are more sensitive to the resolved component and a possible underlying event. The predictions of HERWIG with two different photon PDFs are also shown. The prediction using the GRV set is flat, irrespective of the presence of MI, as expected for a photon PDF lacking a Q^2 dependence. The prediction using the SaS 1D PDF decreases with Q^2 and lies below the data in the low Q^2 region. The measured ratios are also compared

with the predictions of LEPTO in the LDIS region in which this model is applicable. The LEPTO predictions show the contribution to the ratio arising from parton shower effects alone and underestimate the measured ratios in both cases.

In Fig. 4(b), the high-E_T^{jet} data are also compared to the predictions of a NLO pQCD calculation at the parton level using the program JetViP [12]. The renormalisation and factorisation scales were set to $\mathrm{Q}^2 + \left(E_T^{jet}\right)^2$. The calculation includes contributions from a resolved photon component, which are computed using two different sets of photon PDFs: the SaS 1D PDF and the GS96 HO [36] PDF modified to include a Q^2 suppression according to Drees and Godbole [6] (GS96 DG). The JetViP predictions are sensitive to the choice of the photon PDFs but lie well below the data. The magnitude of the hadron-to-parton level corrections has been investigated as a possible source of this discrepancy. The data corrections to parton level were estimated using the MC samples and were found to decrease the measured cross section ratios by approximately 20-30%, which is insufficient to explain the discrepancy.

5 Conclusions

Dijet cross sections, $d\sigma/dx_\gamma^{\mathrm{OBS}}$, have been measured using the longitudinally-invariant k_T jet algorithm as a function of Q^2, for $\mathrm{Q}^2 < 1$ GeV^2, $0.1 < \mathrm{Q}^2 < 0.55$ GeV^2 and $1.5 < \mathrm{Q}^2 < 4.5$ GeV^2. The x_γ^{OBS} dependence of the measured dijet cross sections changes with increasing Q^2. The low-x_γ^{OBS} cross section decreases more rapidly than the high-x_γ^{OBS} cross section as Q^2 increases. This effect is more pronounced for the lower of the two sets of E_T^{jet} cuts.

The shape of the dijet cross sections, $d\sigma/dx_\gamma^{\mathrm{OBS}}$, is compared to the predictions of HERWIG MC for a variety of photon PDFs. None of these models is able to explain the data for both high- and low-E_T^{jet} cuts in all Q^2 ranges.

The ratio $\sigma(x_\gamma^{\mathrm{OBS}} < 0.75)/\sigma(x_\gamma^{\mathrm{OBS}} > 0.75)$ for dijet cross sections decreases as Q^2 increases but remains above the level expected from parton-shower effects alone. This may be interpreted in terms of a resolved photon component which is suppressed as the photon virtuality increases but which remains present up to $\mathrm{Q}^2 = 4.5$ GeV^2 when the photon is probed at the scale $\mu^2 \sim 30$ GeV^2 of these measurements. Within the models available, events at $x_\gamma^{\mathrm{OBS}} < 0.75$ can originate from non-perturbative photon structure or perturbatively-calculable higher-order processes, and are influenced by underlying-event effects especially at low Q^2 and low E_T^{jet}. The features and trends seen in the data are in accord with general expectations. However, none of the LO models, or the NLO calculation examined here, gives a good description of the data across the full kinematic region.

Acknowledgements

The design, construction and installation of the ZEUS detector have been made possible by the ingenuity and dedicated efforts of many people from inside DESY and from the home institutes who are not listed as authors. Their contributions are acknowledged

with great appreciation. The experiment was made possible by the inventiveness and the diligent efforts of the HERA machine group. The strong support and encouragement of the DESY directorate have been invaluable. We would like to thank B. Pötter and G. Kramer for valuable discussions and for providing the NLO calculations. We would also like to thank M. Drees, R. Godbole, B. Harris, M. Klasen and J. Dainton for helpful discussions.

References

[1] H1 Collab., S. Aid et al., Nucl. Phys. B470 (1996) 3;
ZEUS Collab., M. Derrick et al., Z. Phys. C72 (1996) 399;
ZEUS Collab., J. Breitweg et al., Phys. Lett. B407 (1997) 432;
H1 Collab., C. Adloff et al., Nucl. Phys. B497 (1997) 3;
A. Levy, Phys. Lett. B404 (1997) 369.

[2] JADE Collab. W. Bartel et al., Z. Phys. C24 (1984) 231;
TASSO Collab., M. Althoff at al., Z. Phys. C31 (1986) 527;
PLUTO Collab., C. Berger at al., Nucl. Phys. B281 (1987) 365;
TPC/2γ Collab. H. Aihara et al., Z. Phys. C34 (1987) 1;
L3 Collab., M. Acciarri et al., Phys. Lett. B436 (1998) 403;
ALEPH Collab., R. Barate et al., Phys. Lett. B458 (1999) 152;
L3 Collab., M. Acciarri et al., Phys. Lett. B447 (1999) 147;
L3 Collab., M. Acciarri et al., Phys. Lett. B453 (1999) 333.

[3] H1 Collab., T. Ahmed et al., Phys. Lett. B297 (1992) 205;
ZEUS Collab., M. Derrick et al., Phys. Lett. B297 (1992) 404;
H1 Collab., I. Abt et al., Phys. Lett. B314 (1993) 436;
ZEUS Collab., M. Derrick et al., Phys. Lett. B322 (1994) 287;
ZEUS Collab., M. Derrick et al., Phys. Lett. B342 (1995) 417;
ZEUS Collab., M. Derrick et al., Phys. Lett. B348 (1995) 665;
ZEUS Collab., J. Breitweg et al., Eur. Phys. J. C4 (1998) 591;
H1 Collab., C. Adloff et al., Eur. Phys. J. C1 (1998) 97;
ZEUS Collab., J. Breitweg et al., Eur. Phys. J. C11 (1999) 35.

[4] ZEUS Collab., J. Breitweg et al., Eur. Phys. J. C1 (1998) 109.

[5] G. Schuler and T Sjöstrand, Phys. Lett. B376 (1996) 193.

[6] M.Drees and R.Godbole, Phys. Rev. D50 (1994) 3124.

[7] T. Uematsu and T. Walsh, Phys. Lett. B101 (1981) 263;
T. Uematsu and T. Walsh, Nucl. Phys. B199 (1982) 93;
F. Borzumati and G. Schuler, Z. Phys. C58 (1993) 139;
M. Glück, E. Reya and I. Schienbein, Phys. Rev. D60 (1999) 54019.

[8] M. Glück, E. Reya and M. Stratmann, Phys. Rev. D54 (1996) 5515;
D.de Florian, C. Canal and R. Sassot, Z. Phys. C75 (1997) 265;
M. Klasen, G. Kramer and B. Pötter, Eur. Phys. J. C1 (1998) 261.

[9] PLUTO Collab., Ch. Berger et al., Phys. Lett. B142 (1984) 119;
L3 Collab. F. Erné et al., Proc. of Photon 99 Conf., 23-27 May 1999,
Freiburg, Germany (to appear).

[10] H1 Collab., C. Adloff et al., Phys. Lett. B415 (1997) 418.

[11] H1 Collab., C. Adloff et al., DESY-98-205, submitted to Eur. Phys. J. C.

[12] G. Kramer and B. Pötter, Eur. Phys. J. C5 (1998) 665;
B. Pötter, Eur. Phys. J. direct C5 (1999) 1;
B. Pötter, Comp. Phys. Comm. 119 (1999) 4;
B. Pötter, private communication.

[13] ZEUS Collab., M. Derrick et al., Phys. Lett. B293 (1992) 465.

[14] The ZEUS Detector, Status Report 1993, DESY 1993.

[15] M. Derrick et al., Nucl. Instr. and Meth. A309 (1991) 77;
A. Andresen et al., Nucl. Instr. and Meth. A309 (1991) 101;
A. Bernstein et al., Nucl. Instr. and Meth. A336 (1993) 23.

[16] ZEUS Collab., J.Breitweg et al., Phys. Lett. B407 (1997) 432.

[17] N. Harnew et al., Nucl. Instr. and Meth. A279 (1989) 290;
B. Foster et al., Nucl. Phys. B32 (1993) 181(Proc. Suppl.);
B. Foster et al., Nucl. Instr. and Meth. A338 (1994) 254.

[18] ZEUS Collab., M. Derrick et al., Z. Phys. C72 (1996) 47.

[19] ZEUS Collab., J. Breitweg et al., Z. Phys. C74 (1997) 207.

[20] H. Abramowicz, A. Caldwell and R. Sinkus,
Nucl. Instr. and Meth. A365 (1995) 508.

[21] F. Jacquet and A. Blondel, Proceedings, Study of an *ep* facility
for Europe, Hamburg, ed. U. Amaldi, DESY 79-48, (1979) 391.

[22] S. Catani et al., Nucl. Phys. B406 (1993) 187;
S.D. Ellis and D.E. Soper, Phys. Rev. D48 (1993) 3160.

[23] G. Marchesini et al., Comp. Phys. Comm. 67 (1992) 465.

[24] M. Glück, E. Reya and A. Vogt, Phys. Rev. D46 (1992) 1973.

[25] A.D. Martin, W.J. Stirling and R.G. Roberts, Phys. Rev. D50 (1994) 6734.

[26] T. Sjöstrand and M. van Zijl, Phys. Rev. D36 (1987) 2019;
G. Schuler and T. Sjöstrand, Phys. Lett. B300 (1993) 169;
G. Schuler and T. Sjöstrand, Nucl. Phys. B407 (1993) 539;
J.M. Butterworth and J.R. Forshaw, J. Phys. G. 19 (1993) 1657.

[27] J. M. Butterworth, J. R. Forshaw and M. H. Seymour, Z. Phys. C72 (1996) 637.

[28] ZEUS Collab., J. Breitweg et al., Eur. Phys. J. C6 (1999) 239.

[29] Sean Mattingly, 'Virtual Photon Structure with ZEUS at HERA',
Ph.D Thesis, University of Wisconsin - Madison, (1999) (unpublished).

[30] N. Macdonald, 'Structure of the Virtual Photon at HERA',
Ph.D Thesis, University of Glasgow (1999) (unpublished).

[31] ZEUS Collab., M. Derrick et al., Phys. Lett. B342 (1995) 417;
ZEUS Collab., M. Derrick et al., Phys. Lett. B348 (1995) 665.

[32] T. Sjöstrand, Comp. Phys. Comm. 82 (1994) 74.

[33] K. Hagiwara, M. Tanaka and I. Watanabe, Phys. Rev. D51 (1995) 3197.

[34] LEPTO 6.5, G. Ingelman, A. Edin and J. Rathsman,
Comp. Phys. Comm. 101 (1997) 108.

[35] J. Butterworth and R. Taylor , 'A global study of photon induced jet production',
hep-ph/9907394, Proc. of Photon 99 Conf., 23-27 May 1999,
Freiburg, Germany (to appear).

[36] L. Gordon and J.K. Storrow, Nucl. Phys. B489 (1997) 405.

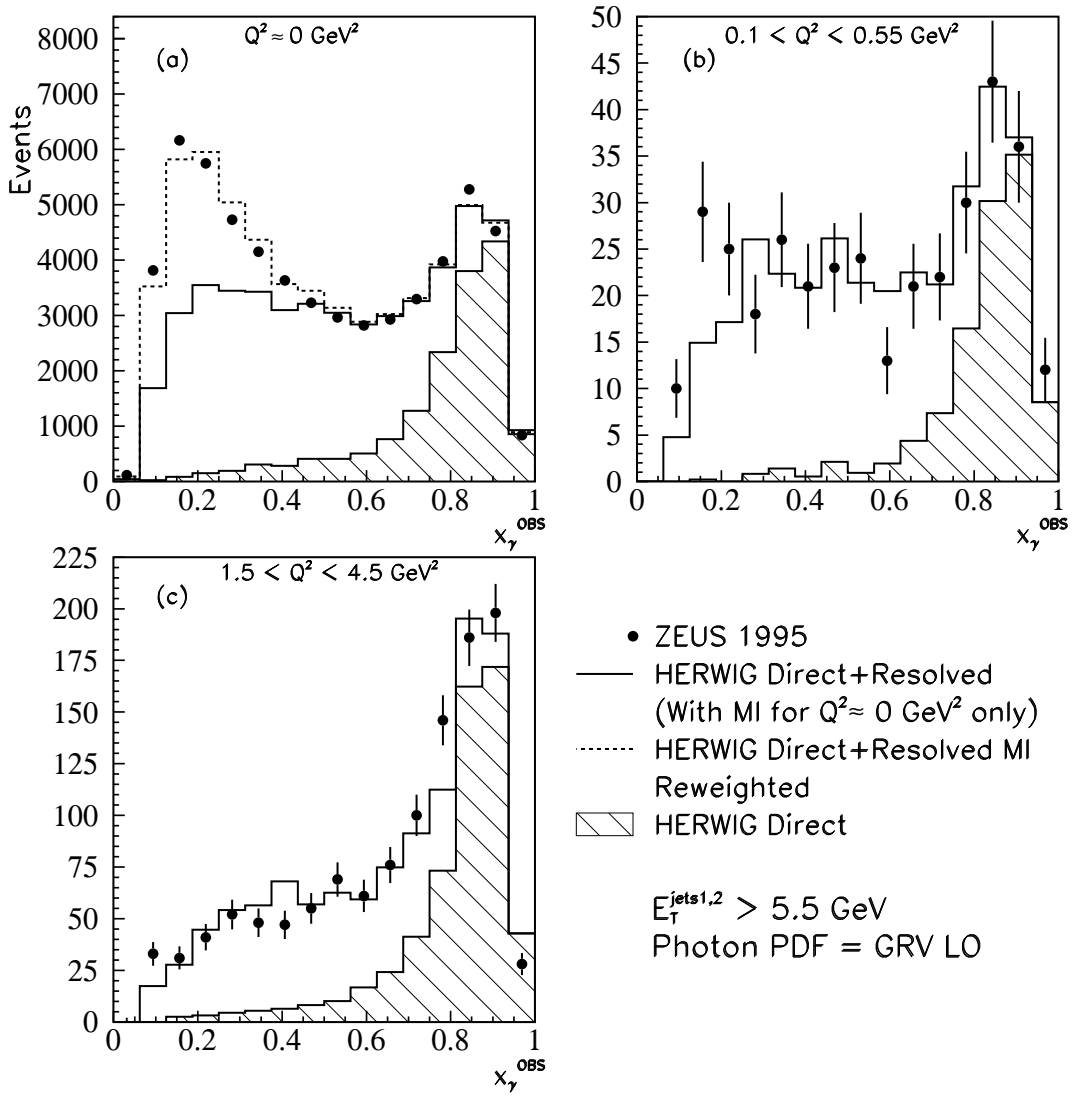

Figure 1: Uncorrected $x_\gamma^{\rm OBS}$ distributions for dijet events selected with the k_T algorithm, for $E_T^{jet} > 5.5$ GeV and $-1.125 < \eta^{jet} < 2.2$, in the ranges: (a) $Q^2 \approx 0$ GeV^2, (b) $0.1 < Q^2 < 0.55$ GeV^2, and (c) $1.5 < Q^2 < 4.5$ GeV^2. The points are the measurements and the solid histograms are the predictions of the HERWIG Monte Carlo. The simulation of multiple parton interactions was used only for the $Q^2 \approx 0$ GeV^2 sample. In (a) the reweighted predictions of HERWIG (dashed histogram) used for the data correction are also shown. The shaded histograms represent the LO-DIR contributions.

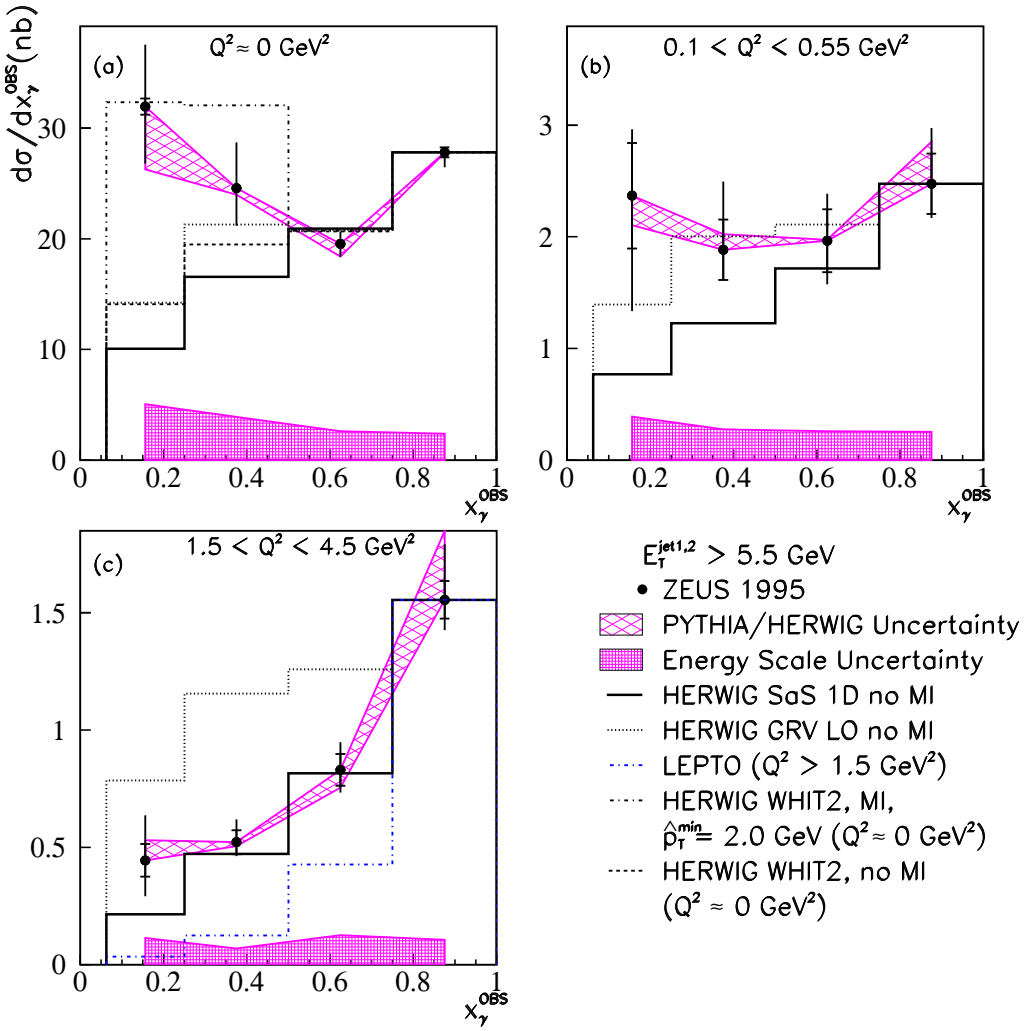

Figure 2: Dijet cross sections, $d\sigma/dx_\gamma^{\rm OBS}$, for jets of hadrons selected with the k_T algorithm in the Q^2 ranges: (a) $Q^2 \approx 0$ GeV^2, (b) $0.1 < Q^2 < 0.55$ GeV^2, (c) $1.5 < Q^2 < 4.5$ GeV^2 for the low E_T^{jet} set of cuts. The points represent the measured cross sections. The inner error bars represent the statistical errors, and the outer are the statistical and uncorrelated systematic errors added in quadrature. The shaded band represents the systematic uncertainty due to the modelling of the jet fragmentation, estimated using PYTHIA. The shaded horizontal band represents the uncertainty due to the CAL energy scale. The full histogram represents the HERWIG predictions without MI using the SaS 1D photon PDFs, and the dotted histogram represents those with the GRV LO real photon PDFs. The predictions of HERWIG without MI using the WHIT2 set (dashed histogram) and with MI for $\hat{p}_T^{\rm min} = 2.0$ GeV (dot–dashed histogram) are shown in (a). The predictions of LEPTO are shown in (c) as the dot-dashed histogram. The LEPTO and HERWIG predictions have been normalised to the $x_\gamma^{\rm OBS} > 0.75$ dijet cross section.

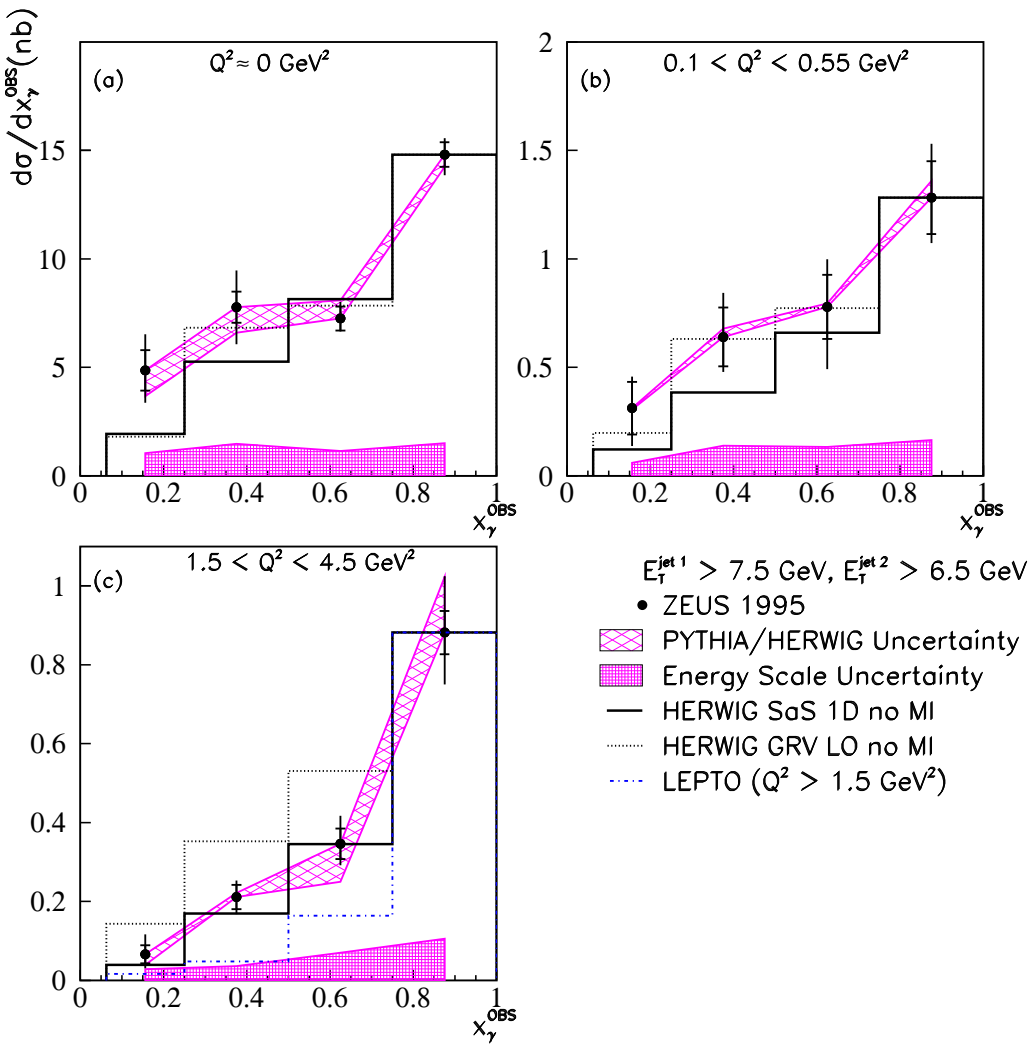

Figure 3: Dijet cross sections, $d\sigma/dx_\gamma^{\rm OBS}$, for jets of hadrons selected with the k_T algorithm in the Q^2 ranges : (a) $Q^2 \approx 0$ GeV^2, (b) $0.1 < Q^2 < 0.55$ GeV^2, (c) $1.5 < Q^2 < 4.5$ GeV^2 for the high E_T^{jet} set of cuts. The points represent the measured cross sections. The inner error bars represent the statistical errors and the outer are the statistical and the uncorrelated systematic errors added in quadrature. The shaded band represents the systematic uncertainty due to the modelling of the jet fragmentation, estimated using PYTHIA. The shaded horizontal band represents the uncertainty due to the CAL energy scale. The full histogram represents the HERWIG prediction without MI using the SaS 1D photon PDFs, and the dotted histogram the GRV LO photon PDFs. The predictions of LEPTO are shown in (c) as the dot-dashed histogram. The LEPTO and HERWIG predictions have been normalised to the $x_\gamma^{\rm OBS} > 0.75$ dijet cross section.

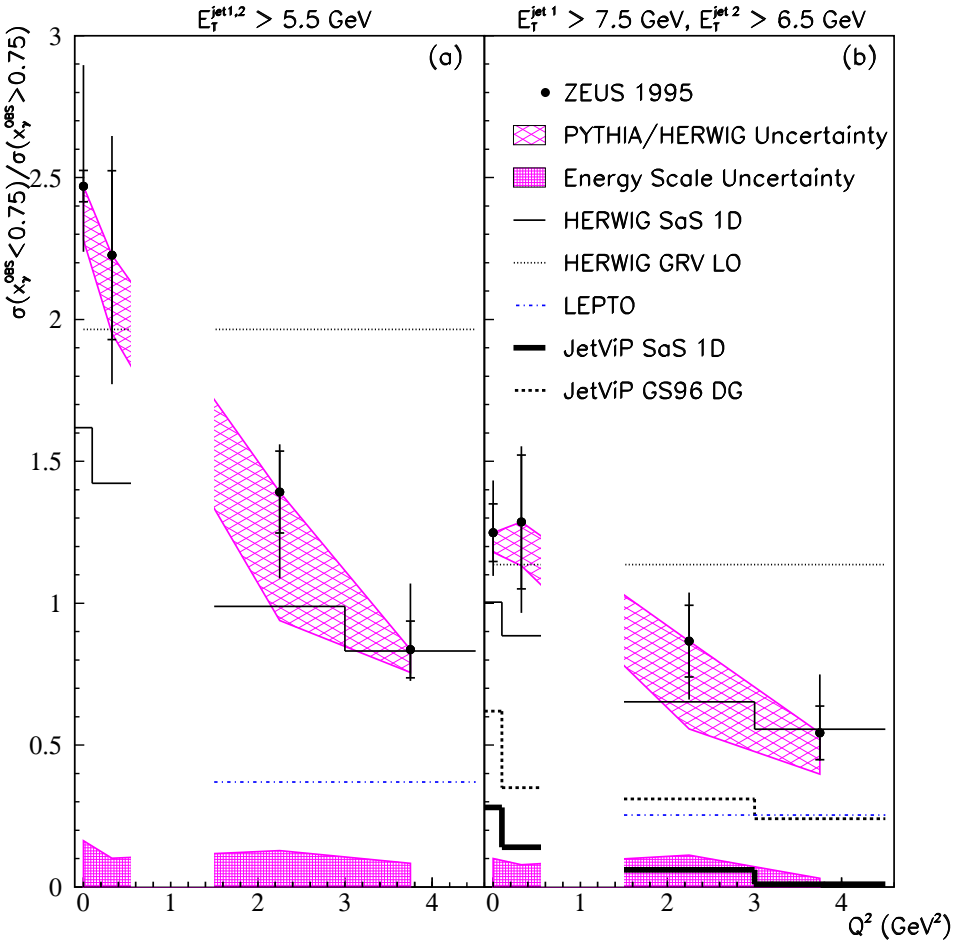

Figure 4: The ratio of dijet cross sections, $\sigma(x_\gamma^{\rm OBS} < 0.75)/\sigma(x_\gamma^{\rm OBS} > 0.75)$, as a function of photon virtuality, Q^2, for dijet events selected using the k_T algorithm. The points represent the ZEUS data. The cross section ratios are shown for both the low (a) and the high (b) E_T^{jet} cuts. The inner error bars represent the statistical errors and the outer are the statistical and systematic errors added in quadrature. The shaded band represents the systematic error due to the uncertainty in modelling the jet fragmentation, estimated using PYTHIA. The shaded horizontal band represents the uncertainty due to the CAL energy scale. Also shown are the predictions of HERWIG without MI for two different choices of photon PDFs: GRV for real photons (dotted histogram) and SaS 1D (full histogram). The LEPTO predictions are shown for $Q^2 > 1.5$ GeV^2 (dot–dashed histogram). The predictions of NLO pQCD calculated using the JetViP program with SaS 1D Photon PDFs are shown as the full histogram and those using GS96 DG are shown as dashed the histogram.